PROPAGATION OF A FLUID-DRIVEN PENNY-SHAPED FRACTURE PARALLEL TO THE FREE-SURFACE OF AN ELASTIC SOLID

Xi Zhang[1] Alexei Savitski[2] Emmanuel Detournay[2] Rob Jeffrey[1]
[1] CSIRO Petroleum, PO Box 3000, Glen Waverley, VIC, Australia
[2] Department of Civil Engineering, University of Minnesota, MN, USA

ABSTRACT

A computational procedure is developed for solving the problem of a penny-shaped fracture propagating parallel to the free-surface of an impermeable elastic solid. The fracture is driven by injection of an incompressible viscous fluid. The crack is modeled as a continuous distribution of dislocation disks associated to normal and shear displacement discontinuities along the fracture. The Green's functions for the elastic half-space are derived based on Eshelby's method for inclusions in infinite isotropic solids and a powerful "reflection" rule devised by Aderogba [1]. The resulting integro-differential equations are solved numerically for the viscosity-dominated regime of fluid-driven crack propagation. The strong non-linear coupling of elasticity and fluid flow is handled by a finite difference scheme, and the time step varies until the chosen increment of crack propagation is satisfied. Numerical results are presented for the crack radius, opening and net pressure as a function of radial distance and time, for the case of a given constant injection rate.

KEYWORDS

Hydraulic Fracture; Elasticity; Green's Functions; Half-Space; Viscosity-Dominated Regime

INTRODUCTION

Hydraulic fracturing is a stimulation technique of underground reservoirs of hydrocarbons, which relies on inducing a fracture in the reservoir rock by injecting a viscous fluid from a borehole. A hydraulic fracture can propagate from the borehole over large distance despite the presence of a confining (compressive) stress, due the internal pressurization by the fracturing fluid. Although most applications of this technique involve deep fractures, there are specific cases where the influence of a free-surface on fracture growth becomes significant or even dominant, as shown in Fig.1. Hydraulic fracture near a free surface has recently been applied to induce rock caving in mining [2]. In such cases, the hydraulic fracture is characterized by a ratio of the fracture radius over the distance from the free surface which can reach order 1 [3].

Knowledge of the Green's functions is crucial to establish the governing equations for the crack problems. In general, the penny-shaped cracks can be modelled by a continuous distribution of dislocations associated to normal and shear displacement discontinuites. By using Eshelby's method, closed-form Green's functions for many dislocation problems have been obtained, see Mura [4]. We present a brief summary of the solutions for a dislocatio loop in an elastic space by means of Eshelby's method. The solutions are then extended to a half-space using the "reflection" rule due to Aderogba [1].

Solutions for fluid-driven fractures are based on integral equations obtained by linear superposition of the Green's functions for dislocation disks along the fracture. The fracture process involves the coupled mechanisms of rock fracturing and flow of an incompressible viscous fluid. It is assumed that the energy dissipated in the creation of new fracture surface is small compared to that expended in viscous flow. This is the so-called viscosity-dominated regime. The corresponding self-similar asymptotic solution at the tip region was given by

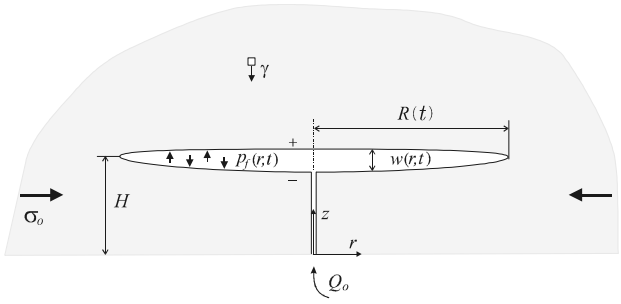

Figure 1: Penny-shaped hydraulic fracture propagating parallel to the free-surface of an elastic half-space

Desroches *et al.* [5]. A numerical algorithm is developed here for simulating the propagation of a hydraulic fracture at a fixed distance from the free surface.

GREEN'S FUNCTIONS FOR A HALF-SPACE

In linear elastic solids, the stresses and displacements can be expressed in terms of the Papkovich-Neuber(P-N) potentials $\{\Phi_i, \Psi\}$ $(i = 1, 3)$,

$$\sigma_{ij} = (\kappa - 1)(\Phi_{j,i} + \Phi_{i,j})/2 + (3 - \kappa)\Phi_{k,k}\delta_{ij}/2 - x_k\Phi_{k,ij} - \Psi_{,ij} \quad (1)$$

$$2\mu u_i = (\kappa + 1)\Phi_i - (x_j\Phi_j + \Psi)_{,i} \quad (2)$$

in which σ_{ij} is the Cauchy stress, ε_{ij} the strain tensor, u_i the displacement vector and μ and ν the material constants, $\kappa = 3 - 4\nu$. Consider a unit point force acting along the x_3-axis at $\mathbf{x}^{'} = (x_1^{'}, x_2^{'}, x_3^{'})$ in an infinite elastic solid. The P-N Potentials are given by

$$\Phi_1 = \Phi_2 = 0, \quad \Phi_3 = c/R, \quad \Psi = -cx_3^{'}/R \quad (3)$$

in which $c = 1/(\kappa + 1)$. In the same way, we can obtain the Green's functions for unit point forces along the x_1 and x_2 directions. In the cylindrical coordinate system, a unit point force in the r (θ) direction can be decomposed into two parts: $f_1 = \cos\theta^{'}(-\sin\theta^{'})$ and $f_2 = \sin\theta^{'}(\cos\theta^{'})$ in the x_1 and x_2 directions. Then the displacements in the Cartesian coordinate system can be obtained by superposition. In a straightforward way, the Green's functions in the cylindrical system can be found by applying a coordinate transformation.

To model a crack, the concept of dislocation loops must be introduced. For an infinitesimal loop, the eigenstrain e_{ij}^T inside the loop can be taken as homogeneous and has the form

$$e_{ij}^T(\mathbf{x}) = -(b_i n_j + b_j n_i)\delta(\mathbf{S} - \mathbf{x})/2 \quad (4)$$

in which $\delta(\mathbf{S} - \mathbf{x})$ is the Dirac delta and b_i the Burgers vector.

When a uniform eigenstrain e_{ij}^T is prescribed within an infinitesimal closed subregion V, the eigenstress σ_{ij}^T can be obtained through Hooke's law

$$\sigma_{ij}^T = 2\mu[\left[e_{ij}^T + \frac{\nu}{1 - 2\nu}e_{kk}^T\delta_{ij}\right] \quad (5)$$

From Eshelby's method, the displacement fields due to the disturbed eigenstresses can be expressed as

$$u_i(\mathbf{x}) = \int_V \sigma_{kl}^T(\mathbf{x}^{'})\frac{\partial}{\partial x_l^{'}}G_{ik}(\mathbf{x}, \mathbf{x}^{'})d\mathbf{x}^{'} \quad (6)$$

see details in [1,4]. Two specific cases are listed below:

1. Opening dislocations: The eigenstresses caused by the eigenstrain e_{zz}^T are

$$\sigma_{rr}^T = \nu P e_{zz}^T, \quad \sigma_{\theta\theta}^T = \nu P e_{zz}^T, \quad \sigma_{zz}^T = (1 - \nu)P e_{zz}^T \quad (7)$$

in which $P = 2\mu/(1 - 2\nu)$.

2. Shearing dislocations: The non-zero eigenstresses can be written as

$$\sigma_{rz}^T = 2\mu e_{rz}^T, \quad \sigma_{zr}^T = 2\mu e_{rz}^T \tag{8}$$

For a dislocation ring, displacements at any point in the space can be obtained by superposition of infinitesimal loops along the ring. It is found that all integrals can be expressed in terms of the Lifschitz-Hankel (L-H) integrals defined in [6]. Here, a modified form of L-H integrals are employed [7]

$$\bar{J}(m,n,p) = (\text{sgn}[\xi])^{m+n+p} J(m,n,p) \tag{9}$$

$$J(m,n,p) = \int_0^\infty J_m(t) J_n(\rho t) e^{-\varpi t} t^p dt \tag{10}$$

where $\rho = r/r', \xi = z/r', \xi' = z'/r'$, r' is the radius of the dislocation ring and $\varpi = \left|\xi - \xi'\right|$. Hence the displacements and the P-N potentials for the opening loop are given by

$$\overline{u}_r = d/r'[-(\kappa-1)/2\bar{J}(0,1,1) + (\xi-\xi')\bar{J}(0,1,2)] \tag{11}$$

$$\overline{u}_z = d/r'[(\kappa+1)/2\bar{J}(0,0,1) + (\xi-\xi')\bar{J}(0,0,2)] \tag{12}$$

with $d = 2\mu/(1+\kappa)$. Substitution of displacements in (2) yields

$$\bar{\Phi}_z^t = d/r' \bar{J}(0,0,1) \tag{13}$$

$$\bar{\Psi}^t = -d[(\kappa-1)/2\bar{J}(0,0,0) + \xi' \bar{J}(0,0,1)] \tag{14}$$

and for shearing loops, we have

$$\overline{u}_r = d/r'[(\kappa+1)\bar{J}(1,1,1) - 2(\xi-\xi')\bar{J}(1,1,2)] \tag{15}$$

$$\overline{u}_z = d/r'[-(\kappa-1)\bar{J}(1,0,1) - 2(\xi-\xi')\bar{J}(1,0,2)] \tag{16}$$

This leads to

$$\bar{\Phi}_z^s = d/r' \bar{J}(1,0,1) \tag{17}$$

$$\bar{\Psi}^s = -d[(\kappa+1)/2\bar{J}(1,0,0) + \xi' \bar{J}(1,0,1)] \tag{18}$$

A very powerful tool developed by Aderogba [1] can be used to connect the solution for an infinite medium and the one for a bonded semi-infinite medium. A special case is considered here, i.e. Φ_r and Φ_θ vanish. Hence,

$$\Phi_z = \Phi_z^0(r,\theta,z) + \kappa\Phi_z^0(r,\theta,-z) + 2\frac{\partial}{\partial z}\Psi^0(r,\theta,-z) \tag{19}$$

$$\Psi = \Psi^0(r,\theta,z) + \kappa\Psi^0(r,\theta,-z) + (\kappa^2-1)/2 \int \Phi_z^0(r,\theta,-z)dz \tag{20}$$

Substitution of (13,14) in the above equations leads to the P-N potentials for half-space problems

$$\hat{\Phi}_z^t = d/r'[\bar{J}^{(1)}(0,0,1) - \bar{J}^{(2)}(0,0,1) - 2\xi' \bar{J}^{(2)}(0,0,2)] \tag{21}$$

$$\hat{\Psi}^t = d[-\frac{\kappa-1}{2}\bar{J}^{(1)}(0,0,0) - \xi' \bar{J}^{(1)}(0,0,1) + \frac{\kappa-1}{2}\bar{J}^{(2)}(0,0,0) + \kappa\xi' \bar{J}^{(2)}(0,0,1)] \tag{22}$$

for opening dislocation rings. Also, we can obtained the P-N potentials for shearing dislocation rings

$$\hat{\Phi}_z^s = d/r'[\bar{J}^{(1)}(1,0,1) - \bar{J}^{(2)}(1,0,1) + 2\xi' \bar{J}^{(2)}(1,0,2)] \tag{23}$$

$$\hat{\Psi}^s = d[-\frac{\kappa+1}{2}\bar{J}^{(1)}(1,0,0) - \xi' \bar{J}^{(1)}(1,0,1) + \frac{\kappa+1}{2}\bar{J}^{(2)}(1,0,0) - \kappa\xi' \bar{J}^{(2)}(1,0,1)] \tag{24}$$

in which $\bar{J}^{(1)}(m,n,p)$ and $\bar{J}^{(2)}(m,n,p)$ represent the modified L-H integrals for the dislocation ring and its image.

Now let us consider a dislocation disk. For the opening dislocations, we assumed a uniform distribution of displacement discontinuity on the whole circular dislocation disk with a radius R. On the other hand, since there is no shear displacement at the centre,we assumed that the shear displacement discontinuity is proportional to the distance from the center; then the Burgers vector is defined as

$$\bar{b}_{rz} = r^{'} b_{rz}/R \tag{25}$$

After integration from 0 to R, the normal stress and shear stresses for the opening case are given by

$$\tilde{\sigma}^t_{zz} = -\bar{J}^{(1)}(1,0,1) - (\xi - \xi^{'})\bar{J}^{(1)}(1,0,2) + \bar{J}^{(2)}(1,0,1) + (\xi + \xi^{'})\bar{J}^{(2)}(1,0,2) + 2\xi\xi^{'}\bar{J}^{(2)}(1,0,3) \tag{26}$$

$$\tilde{\sigma}^t_{rz} = -(\xi - \xi^{'})\bar{J}^{(1)}(1,1,2) + (\xi - \xi^{'})\bar{J}^{(2)}(1,1,2) + 2\xi\xi^{'}\bar{J}^{(2)}(1,1,3) \tag{27}$$

and for the shear case

$$\tilde{\sigma}^s_{zz} = -(\xi - \xi^{'})\bar{J}^{(1)}(2,0,2) + (\xi - \xi^{'})\bar{J}^{(2)}(2,0,2) - 2\xi\xi^{'}\bar{J}^{(2)}(2,0,3) \tag{28}$$

$$\tilde{\sigma}^s_{rz} = \bar{J}^{(1)}(2,1,1) - (\xi - \xi^{'})\bar{J}^{(1)}(2,1,2) - \bar{J}^{(2)}(2,1,1) + (\xi + \xi^{'})\bar{J}^{(2)}(2,1,2) - 2\xi\xi^{'}\bar{J}^{(2)}(2,1,3) \tag{29}$$

in which $\tilde{\sigma}^{t(s)}_{ij} = 4R\sigma^{t(s)}_{ij}/E^{'}$, $E^{'} = E/(1-\nu^2)$.

GOVERNING EQUATIONS AND SCALING

Using the singular solutions for dislocation loops, two singular integral equations can be established

$$\int_0^R G_{nn}\left(\frac{r}{R},\frac{s}{R};\mathcal{R}\right) d_n(s,t)ds + \int_0^R G_{ns}\left(\frac{r}{R},\frac{s}{R};\mathcal{R}\right) d_s(s,t)ds = -\frac{R}{E'}p(r,t) \tag{30}$$

$$\int_0^R G_{sn}\left(\frac{r}{R},\frac{s}{R};\mathcal{R}\right) d_n(s,t)ds + \int_0^R G_{ss}\left(\frac{r}{R},\frac{s}{R};\mathcal{R}\right) d_s(s,t)ds = 0 \tag{31}$$

in which $\mathcal{R} = H/R$, H the crack depth; $G_{nn} = \tilde{\sigma}^t_{zz}/4$, $G_{ns} = \tilde{\sigma}^s_{zz}/4$, $G_{sn} = \tilde{\sigma}^t_{rz}/4$ and $G_{ss} = \tilde{\sigma}^s_{rz}/4$; d_n and d_s are dislocation densities. The above equations are rearranged in terms of the opening w and shear displacement discontinuity u as

$$\mathcal{H}\{w;\mathcal{R}\} = p(r,t)/E' \tag{32}$$

The equation governing the flow of viscous fluid in the fracture [8] is

$$\frac{\partial w}{\partial t} = \frac{1}{12\gamma r}\frac{\partial}{\partial r}\left(r w^3 \frac{\partial p}{\partial r}\right) \tag{33}$$

in which γ is the fluid viscosity. The condition that the fracture is in mobile equilibrium at the tip $r = R(t)$, $K_I = K_{Ic}$, can be expressed as

$$w \simeq \frac{K'}{E'}(R-r)^{1/2} \qquad R - r \ll R \tag{34}$$

Besides the condition $w(R,t) = 0$, the boundary conditions at the fracture inlet $r = 0$ are

$$q(R,t) = 0 \quad \text{and} \quad 2\pi \lim_{r\to 0} rq = Q_o \tag{35}$$

It follows from the above equation that $q \sim O(1/r)$ near the source and $p \sim -\ln r$. Alternatively, the source can be taken into account by the global continuity equation

$$2\pi \int_0^R r\, w \mathrm{d}r = Q_o t \tag{36}$$

Introduce an arbitrary time scale T. Given an injection rate Q_o, a fixed reference length $\bar{L}_\mu$ is defined as

$$\bar{L}_\mu = \left(\frac{E' Q^3 T^4}{\gamma'}\right)^{1/9} \tag{37}$$

in which $\gamma' = 12\gamma$. After defining the dimensionless time $\tau = t/T$ and radial coordinate $\xi = r/\bar{L}_\mu$, the dimensionless fracture radius $\chi(\tau)$ ($0 \leq \xi \leq \bar{\chi}$), openings $\bar{\Omega}(\xi,\tau)$ and $\bar{\Xi}(\xi,\tau)$, and pressure $\bar{\Pi}(\xi,\tau)$ are introduced as follows [9]

$$\chi = R/\bar{L}_\mu \qquad \bar{\Omega} = w/\bar{\varepsilon}_\mu \bar{L}_\mu \qquad \bar{\Xi} = u/\bar{\varepsilon}_\mu \bar{L}_\mu \qquad \bar{\Pi} = p/\bar{\varepsilon}_\mu E' \tag{38}$$

where the small number $\bar{\varepsilon}_\mu = \varepsilon_\mu(T)$ is defined as

$$\bar{\varepsilon}_\mu = (\gamma'/E'T)^{1/3} \tag{39}$$

We can now formulate the set of equations to be solved for $\bar{\Omega}(\xi,\tau)$ and $\chi(\tau)$. By expressing $\bar{\Pi}$ in (33) in terms of $\bar{\Omega}$ using (32), a single integro-differential equation for $\bar{\Omega}$ can be formulated

$$\frac{\partial \bar{\Omega}}{\partial \tau} = \frac{1}{\xi}\frac{\partial}{\partial \xi}\left(\xi \bar{\Omega}^3 \frac{\partial}{\partial \xi}\mathcal{H}\{\bar{\Omega};\mathcal{R}\}\right) \tag{40}$$

The inlet boundary condition is translated in terms of the opening

$$\xi \bar{\Omega}^3 \frac{\partial}{\partial \xi}\mathcal{H}\{\bar{\Omega};\mathcal{R}\}\Big|_{\xi=0} = \frac{1}{2\pi} \tag{41}$$

Finally, the tip behavior of the opening is given by the zero-toughness asymptote [4]

$$\bar{\Omega} = 2^{1/3}3^{5/6}\dot{\chi}^{1/3}(\chi-\xi)^{2/3} \qquad 1-\xi/\chi \ll 1 \tag{42}$$

NUMERICAL ALGORITHM

We outline here the algorithm devised by Savitski [10] to construct the self-similar zero-toughness solution ($\mathcal{R} = 0$). Minor modifications were required here to solve the half-space crack problems. The numerical algorithm is based on a fixed grid with a constant element size $\Delta\xi$, and a variable time step $\Delta\tau$. At each step, the radius is increased by a fixed increment of size $\Delta\xi$ corresponding to an initially unknown time step $\Delta\tau$. After each radius increment $\Delta\xi$, the time step $\Delta\tau$ and the opening $\bar{\Omega}$ have to be calculated using a discretized form of (40-42). The calculations are started with an initial crack radius $\chi_{\min} = 5\Delta\xi$, and assuming the initial crack aperture to correspond to the solution for $\mathcal{R} = 0$. The computations are carried out until the fracture radius reaches a predetermined length $\chi_{\max} = N_{\max}\Delta\xi$.

A combination of a finite difference scheme and the displacement discontinuity method [11] is used to solve numerically (40-42). The following description relies on two indices: the subscript i to denote the nodes at the center of the spatial elements, and the superscript m for the time index. Also, the current number of active elements at time step m is denoted by N. Hence, $\bar{\Omega}_i^m = \bar{\Omega}(\xi_i,\tau_m)$ with $\xi_i = (i-1/2)\Delta\xi$ and $i = 1, N$; also $\bar{\chi}(\tau_m) = N\Delta\xi$.

The discretized form of (40) can now be written as

$$\frac{\bar{\Omega}_i^m - \bar{\Omega}_i^{m-1}}{\Delta\tau} = \frac{1}{(\Delta\xi)^2}K_{ij}\left(\alpha_{\text{op}}\cdot\bar{\Omega}_j^m + (1-\alpha_{\text{op}})\bar{\Omega}_j^{m-1}\right) + d_i, \qquad i = 1, N \tag{43}$$

where the coefficient α_{op} takes values between 0 (explicit) and 1 (implicit). The source term $d_i = 0$ for all nodes, except for the first one at the well $d_1 = 1/2\pi\Delta\xi$. The matrix $\mathbf{K}$ is defined as

$$K_{ij} = a_i M_{i-1,j} - (a_i + b_i)M_{i,j} + b_i M_{i+1,j} \tag{44}$$

where $\mathbf{M}$ is the elasticity matrix and $\mathbf{a}$, $\mathbf{b}$ the vectors of coefficients; see Savitski [10] for details.

The time step is the solution of the asymptotic equation (42) discretized as

$$\bar{\Omega}_{N+1-i} = 2^{1/3}3^{5/6}\left(\frac{\Delta\xi}{\Delta\tau}\right)^{1/3}\left[\Delta\xi\left(i-\frac{1}{2}\right)\right]^{2/3} \tag{45}$$

Therefore, the time step $\Delta\tau$ can be calculated as

$$\Delta\tau = \frac{1}{N_{\text{tip}}}2\cdot 3^{5/2}(\Delta\xi)^3\sum_{i=1}^{N_{\text{tip}}}\frac{(i-1/2)^2}{(\Omega_{N+1-i})^3} \tag{46}$$

where N_{tip} is the number of nodes taken in the near tip region of the fracture dominated by the asymptotic behavior. Only one node near the tip can be used at the beginning of the simulation, when N is small. As the fracture propagates, more and more elements fall within that region and N_{tip} can be increased.

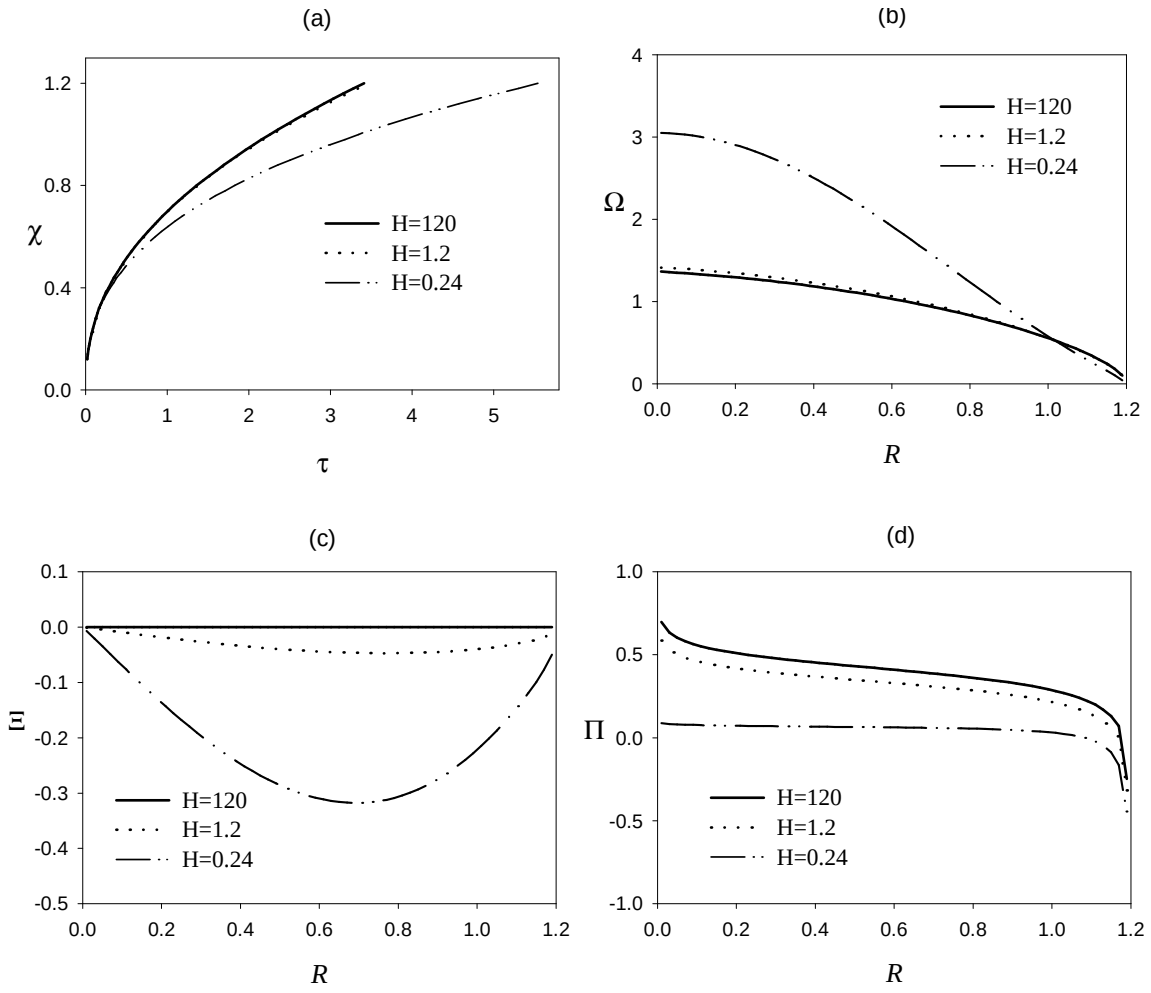

Figure 2: Dimensionless fracture properties at different crack depths, (a) Radius; (b) Opening; (c) Shearing and (d) Pressure.

RESULTS

Computations were performed using $\Delta\xi = 0.02$ and $N_{\max} = 60$. Hence $\chi_{\max} = 1.2$. Figure 2 provides the evolution of the fracture radius, the normal and shear discontinuity and the net pressure along the fracture for three difference crack depths $H = 120,\ 1.2,\ 0.6$. The evolution of the opening and pressure is given at the maximum crack radius $\chi_{\max}$. The expected singular distribution of the net pressure is evident in Fig. 2d. The effect of the free surface on the viscosity-dominated solution can also be observed in Fig. 2: the influence of the free surface is responsible for a larger opening, a smaller length of the fracture, and a smaller inlet pressure at a given time (corresponding to a given volume of fluid injected).

REFERENCES

1. Aderogba, K. (1977) *Phil. Mag.* 35,281
2. Jeffrey, R.G. and Mills, K. W. (2000) In: *Pacific Rocks 2000*, pp. 423-430, Balkema.
3. Pollard, D. and Hozhausen, G. (1979) *Tectonophysics*, 53, 27.
4. Mura, T. (1987) *Micromechanics of Defects in Solids*, 2nd ed. Martenus Nijhoff, Dordrecht.
5. Desroches, J. E., Detournay, E., Lenoach, B., Papanastasiou, P., Pearson, J. R. A., Thiercelin, M, and Cheng, A. H.-D. (1994) *Proc. Roy. Soc. London, Ser. A* A447, 39.
6. Eason, G., Noble, B. and Sneddon, I. (1955) *Phil. Mag. Roy. Soc. London, Ser A* 247, 529.
7. Korsunsky, A. M. (1995) *J. Mech. Phys. Solids* 43, 1221.
8. Batchelor, G. K. (1967) *An Introduction to Fluid Mechanics*, Cambridge University Press.
9. Detournay, E. (2001) In: *Computer Methods an d Advances in Geomechanics*, pp. 1277-1288, Balkema.
10. Savitski, A. (2000) Ph. D. Thesis, University of Minnesota.
11. Crouch, S. and Starfield, A. (1983) *Boundary Element Methods in Solid Mechanics*, George Allen & Unwin.